NIH Public Access
Author Manuscript
Structure. Author manuscript; available in PMC 2010 August 12.

Published in final edited form as:
Structure. 2009 August 12; 17(8): 1137–1147. doi:10.1016/j.str.2009.06.011.

A Tetrahedral Transition State at the Active Sites of the 20S Proteasome is Coupled to Opening of the α-Ring Channel

Pawel A. Osmulski[1], **Mark Hochstrasser**[2], and **Maria Gaczynska**[1,*]

[1]Institute of Biotechnology, University of Texas Health Science Center at San Antonio, 15355 Lambda Dr., San Antonio, TX 78245, USA

[2]Yale University, Department of Molecular Biophysics & Biochemistry, 266 Whitney Ave, New Haven, CT 06520-8114, USA

Summary

Intrinsic conformational transitions contribute to the catalytic action of many enzymes. Here we use a single-molecule approach to demonstrate how such transitions are linked to the catalytic sites of the eukaryotic proteasome, an essential protease of the ubiquitin pathway. The active sites of the cylindrical proteasomal core particle (CP) are located in a central chamber accessible through gated entry channels. By atomic force microscopy (AFM), we found continual alternation between open and closed gate conformations. We analyzed the relative abundance of these conformers in wild-type and mutated yeast CPs upon exposure to substrates or inhibitors. Our data indicate that the dynamic gate can be opened by allosteric coupling to a tetrahedral transition state at any of the working active centers. The results point to the N^{α}-amine of the N-terminal active site threonyl residue as the major effector group responsible for triggering the essential conformational switch.

Introduction

Local and global conformational fluctuations are an intrinsic property of proteins (Henzler-Wildman et al., 2007). Conformational diversity in a single protein is defined by the ligand-independent presence of more than one conformational state (Bahar et al., 2007). Such intrinsic dynamics are postulated to determine catalytic functions and allosteric behavior, broadly understood as a coupling of conformational changes between two widely separated sites (Gunasekaran et al., 2004; Henzler-Wildman et al., 2007). Methods such as NMR, hydrogen/deuterium exchange and molecular modeling based on crystal structures have helped to advance our knowledge of the role of enzyme dynamics in catalysis (Dodson et al., 2008; Henzler-Wildman et al., 2007; Liu and Konermann, 2008). For large multi-component complexes, detailed analysis of the relationship between structural dynamics and activity is far from trivial. In such cases cryo-electron microscopy, atomic force microscopy (AFM) or fluorescence resonance energy transfer have allowed the detection of allosteric transitions (da Fonseca and Morris, 2008; Osmulski and Gaczynska, 2002; Tang et al., 2007). Such methods are also capable of determining whether a ligand-induced change in enzyme activity is best described by conformational selectivity and population-shift, in which the relative fractions of

© 2009 Elsevier Inc. All rights reserved.

*Contact: gaczynska@uthscsa.edu, tel. (210) 567-7262; fax (210) 567-7269.

Publisher's Disclaimer: This is a PDF file of an unedited manuscript that has been accepted for publication. As a service to our customers we are providing this early version of the manuscript. The manuscript will undergo copyediting, typesetting, and review of the resulting proof before it is published in its final citable form. Please note that during the production process errors may be discovered which could affect the content, and all legal disclaimers that apply to the journal pertain.

NIH-PA Author Manuscript
NIH-PA Author Manuscript
NIH-PA Author Manuscript

NIH-PA Author Manuscript

NIH-PA Author Manuscript

NIH-PA Author Manuscript

pre-existing conformational isomers are redistributed, or by induced fit, where an effector molecule directly induces a conformational change in the bound protein (Nevo et al., 2004).

Here we analyze the link between conformational dynamics and enzyme activity in the large hetero-oligomeric 20S proteasome. Most of the regulated degradation of intracellular proteins in eukaryotes occurs through the ubiquitin-proteasome system. Substrates are polyubiquitinated, and the tagged proteins are then degraded by the 26S proteasome, which is composed of a 20S proteasome catalytic core particle (CP) capped at each end by a 19S regulatory particle (RP) (Glickman and Ciechanover, 2002). The latter confers energy- and ubiquitin-dependence on substrate proteolysis. The CP alone is able to degrade small peptides and unfolded proteins or disordered loops in native proteins (Liu et al., 2003).

The 20S proteasome (700 kDa) is made of four stacked heptameric rings, which in eukaryotes assemble from 14 different but related α and β subunits. The rings have an α-β-β-α arrangement, with the outer a rings providing attachment sites on their outer surface (the α face) for the RPs or other regulatory modules; the α-ring forms a gate across the entrance to a central channel leading to the inner catalytic chamber (Groll et al., 1997, 2000a) (Figure 1A). This chamber is formed by the β rings and conceals three pairs of active sites: of the seven β subunits in eukaryotes, only three bear proteolytic active sites: β1, β2 and β5. The proteasome has been characterized as having chymotrypsin-like (ChT-L), trypsin-like (T-L) and postglutamyl peptide-hydrolyzing (PGPH; post-acidic, caspase-like) activities toward small peptide substrates. By mutational analysis in the yeast *Saccharomyces cerevisiae*, the β5 (Doa3/Pre2/Prg1), β2 (Pup1) and β1 (Pre3) subunits, respectively, are responsible for these peptidase activities (Arendt and Hochstrasser, 1997; Chen and Hochstrasser, 1996; Heinemeyer et al., 1997). All active β subunits are synthesized with an N-terminal propeptide, which is autoprocessed during proteasome assembly to free an N-terminal amine, ready to serve as a base for a nucleophilic hydroxyl of the catalytic Thr1 residue (Chen and Hochstrasser, 1996; Schmidtke et al., 1996; Seemuller et al., 1996). Mutation of this Thr residue blocks subunit processing; the propeptide fragment that remains in the mutant prevents both substrate binding and catalysis at the affected active center.

Mounting evidence suggests that the proteasome is an allosteric enzyme. The examples of presumed allostery include interactions between catalytic centers and putative distal substrate-binding sites and routes from the α face to active sites upon binding distinct activator complexes (Rechsteiner and Hill, 2005; Schmidtke et al., 2000). The most intriguing cases describe apparent allosteric coupling between the catalytic chamber and the interface between the CP and RP. In a recent study, binding of a competitive inhibitor to an active site was correlated with increased stability of the CP-RP complex (Kleijnen et al., 2007). Coupling between degradation and the dynamic structure of the a ring was also apparent in our earlier AFM–based analysis of *S. pombe* proteasomes, where we reported shifts in the partitioning between open and closed conformations of the α-ring upon addition of substrates (Osmulski and Gaczynska, 2000, 2002).

The structures of open and closed conformations are known in great detail from X-ray crystallography (Groll et al. 2000a, Whitby et al., 2000) (Figure 1A). The gate responsible for opening and closing the outer pore is formed by N-terminal tails of a subset of a subunits, which either lock together (“closed gate”) or move upward in a concerted fashion (“open gate”) (Forster et al., 2003). The gate is closed in crystal structures of wild-type yeast CP. Such proteasomes in solution are “latent”: they have relatively low, albeit measurable, peptidase activity (Bajorek et al., 2003). Activity is elevated many-fold by opening the gate by, for example, binding regulatory protein modules such as the RP to the α ring or by mutational removal of parts of the gate (Groll et al., 2000a; Smith et al., 2007; Forster et al., 2003). Gate opening may also result from interactions of the CP with substrates – either at the active sites

NIH-PA Author Manuscript

NIH-PA Author Manuscript

NIH-PA Author Manuscript

or elsewhere (Kisselev et al., 2002; Liu et al., 2003; Osmulski and Gaczynska, 2000, 2002). The dynamics of the area surrounding the entrance to the central channel in archaeal proteasomes was recently shown by NMR (Sprangers and Kay, 2007). What remains obscure, however, is the nature of the initiating triggers for these structural changes and the allosteric pathways by which they are transmitted.

Key Findings

In this study, we examined the relationship between proteolytic active-site engagement and the conformational state of the α-ring gate in 20S proteasomes purified from *S. cerevisiae*. Atomic force microscopy (AFM) is a type of single-molecule analysis that can be performed in aqueous media that mimic physiological conditions. Using AFM, we observed a strict correlation between specific states of the β-subunit active centers and gate opening or closing in the α-ring. Our data suggest that each active center in the catalytic chamber is allosterically coupled to the α-ring gate, with a tetrahedral transition state at an active center serving as the likely trigger for gate opening (or for inhibiting its closing). Here we propose a model of a dynamic α-ring gate, in which active centers influence the gate by biasing a pre-existing equilibrium of conformational states. Such a dynamic gate allows access of substrate to the catalytic chamber even without the attachment of the RP or other proteasomal activators. This is consistent with the observation that free 20S proteasomes exhibit physiologically relevant catalytic activity *in vivo* (Liu et al., 2003).

RESULTS

AFM detects an equilibrium of conformational states in latent yeast 20S proteasomes

We examined the topography of latent 20S yeast proteasomes in aqueous buffer under nondestructive conditions with tapping mode AFM, using experimental conditions described previously (Osmulski and Gaczynska, 2000, 2002) and in Supplemental Data. The topography of the particles was consistent with the CP cylinders either standing on their α–ring ends (top-view orientation; majority of particles; Figure 1B, Figure S1A–C) or lying on their sides (side view; Figure S1D). For both orientations, the particles showed a cylinder diameter of about 8–12 nm and a cylinder length of 13–17 nm, which agreed well with crystallographic (Groll et al., 1997) and electron microscopic (da Fonseca and Morris, 2008) data for the 20S proteasome and with our previous AFM data (Gaczynska and Osmulski, 2008) .

Figure 1A–C shows AFM images of *S. cerevisiae* CPs standing on their α-ring ends (top view) in two distinct conformations: either they presented a smooth, cone-shaped apical end (“closed”) or a crater-like depression in the middle (“open”). As in our previous studies, we classified the molecules on the basis of the shape of the median sections of the α-rings (Figure 1B). Individual proteasomes were observed to alternate between the open and closed states on the mica surface (see Supplemental Data). We confirmed the presence of two conformers with multiple species (Gaczynska and Osmulski, 2008) and determined that approximately 25% of wild-type *S. cerevisiae* proteasomes imaged without addition of a ligand were present in the open state, and 75% in the closed state (Table 1).

A substrate induces a shift toward the open 20S proteasome conformation

The distribution of open and closed conformers did not always match the 1:3 ratio noted above. As in our previous studies with *S. pombe* proteasomes (Osmulski and Gaczynska, 2000), in *S. cerevisiae* particles this ratio inverted to a ~3:1 ratio of open-to-closed conformers when we added a model peptide substrate for any of the three active centers (Figure 1C). Specifically, the percent of open particles in the presence of a substrate for the ChT-L site (β5) was 73.9% ± 3.1%, for the T-L site (β2) 74.5% ± 2.8%, and for the PGPH site (β1) 75.7% ± 2.3% (200–500 top-view particles each, from 8–20 fields). The similar observation with *S. pombe*

NIH-PA Author Manuscript

NIH-PA Author Manuscript

NIH-PA Author Manuscript

proteasomes had prompted us to hypothesize that the catalytic act promoted channel opening (Osmulski and Gaczynska, 2000).

To confirm the coupling between catalytic sites and α-ring conformational changes, we tested if a functional active center was necessary to change the distribution of conformers upon addition of substrate. For this purpose, we initially analyzed the effect of mutating each active site Thr1 to Ala. Strikingly, disruption of the β1, β2 or β5 active sites only blocked α-ring channel opening when a model peptide substrate specific for the disabled site was used (Figure 2A). Substrates of the remaining intact sites continued to stimulate high levels of the open conformers, and the basal distributions of conformers were the same as that of the wild-type proteasome. Therefore, inactivation of each active site specifically disrupts the shift toward the open channel conformation normally induced by a peptide substrate specific to that site.

Formation of a tetrahedral complex correlates with proteasome channel opening

Next we attempted to determine which step(s) of the proteolytic catalytic cycle triggers α-ring channel opening. In particular, we considered substrate binding at active sites or other sites, threonine acylation and formation of a tetrahedral intermediate (Figure 3). Although all three analyzed active site mutants lacked the essential Thr1 residue in their respective active sites, a potentially important difference existed between them. For the β1 and β2 T1A substitutions, the mutations were introduced into the full-length precursor forms of these subunits, which causes a precursor processing defect (Arendt and Hochstrasser, 1997). As a result, a residual propeptide (leader sequence, LS) is left in the substrate-binding pocket, as was shown in crystal structure of the β1T1A proteasome (Arendt and Hochstrasser, 1997;Groll et al., 1997). The analogous mutation in the β5 precursor is lethal, but if the Ala1 mutation is introduced into β5ΔLS (propeptide deleted) in cells with the propeptide expressed *in trans*, proteasome assembly can take place and cells survive (Chen and Hochstrasser, 1996). Hence, a β5ΔLS-T1A mutant was analyzed here, resulting in a β5 substrate-binding pocket that should be fully accessible. Despite these differences in binding-pocket occupancy in the three active-site mutant proteasomes, all the particles behaved analogously in response to substrate peptides (Figure 2A). These data suggest that some step associated with substrate cleavage, rather than peptide binding *per se* (at either the active site or elsewhere in the proteasome), is necessary for channel opening.

Based on this preliminary inference, we began to dissect how altering components of a proteasome active center or catalytic events at that site affect the distribution of α-ring conformers. Each active center includes a Thr1-based catalytic dyad with its hydroxyl side chain acting as the attacking nucleophile and α-amino group as general base (Figure 3). A substrate binding pocket and water molecules are also essential components of the active site (Groll et al., 1997). Analogous to serine proteases, the proteasomal catalytic cycle most probably consists of the following steps: (1) nucleophilic attack by the Thr1 hydroxyl on the carbonyl of the peptide bond with transfer of the hydroxyl proton through a bridging water to the N^{α}-amino group; (2) rearrangement of a tetrahedral intermediate to form a covalent acyl intermediate and release of the first product; (3) nucleophilic attack of a water molecule on the carbonyl group esterified to Thr1, leading to formation of a second tetrahedral complex; and (4) rearrangement of the complex and release of the final product (Figure 3) (Osmulski et al., 2009). We addressed the state of the catalytic dyad and the formation of a tetrahedral complex in relation to channel opening using mechanistically distinct active-site inhibitors and yeast mutants.

Peptide epoxyketones constitute a family of highly specific and irreversible inhibitors of the proteasome, forming a covalent morpholino adduct with the active site Thr1 (Supplemental Data, Figure S2). Chemically, they engage both the hydroxyl and α-amino group of the threonyl residue (Elofsson et al., 1999; Groll et al., 2000b). To test their effects on proteasome

NIH-PA Author Manuscript

NIH-PA Author Manuscript

NIH-PA Author Manuscript

conformational switching, the epoxyketone compounds epoxomicin (directed primarily toward β5), YU101 (specific for β5) and YU102 (directed primarily toward β1) were used at concentrations sufficient to block the single favored active center (Table 1, experiments 1–4) (Elofsson et al., 1999; Myung et al., 2001). Strikingly, inhibitor treatments shifted the fraction of open conformers detected in AFM images to as high as 96%. The targeted active center, however, had to be intact in order to support the conformational switch (Table 1, experiments 5–7). Mutant proteasomes with Thr1 of β1 replaced by Ala failed to shift to a high fraction of open conformers upon their treatment with the β1-specific inhibitor YU102. In contrast, the conformational shift was preserved in b1T1A mutant proteasomes treated with an inhibitor targeting the β5 active centers (YU101). Since no product is released by proteasomes blocked with epoxyketones, the conformational shift cannot be due to the release of peptide products. These results supported the possibility that an interaction of a substrate with at least some component of the active center shifts proteasomes to the open state.

Following this lead, we compared the effects of other proteasome inhibitors that form chemically distinct adducts with the hydroxyl of Thr1. First, we tested Z-LLL-VS, a vinyl-sulfone peptide derivative that irreversibly inhibits the β5 active center as its primary target. Peptide vinyl sulfones attack the hydroxyl of Thr1 residue, forming an ether adduct, but do not react with the α-amino group (Figure S2) (Bogyo et al., 1997). In contrast to epoxyketone addition, treatment of proteasomes with Z-LLL-VS did not lead to α-ring opening (Table 1, experiment 8). A similar result was obtained with *clasto*-lactacystin β-lactone, which also reacts with the hydroxyl group but not with the α-amino group (Table 1, experiment 9; Figure S2). The β-lactone forms an ester adduct analogous to the acyl intermediate in the proteasome reaction cycle (Corey et al., 1999;). Therefore, the AFM data argue against an acyl intermediate as a key allosteric effector for α-ring opening.

Next, we inspected proteasomes treated with the boronic acid peptide derivatives bortezomib [pyrazylcarbonyl-FL-B$(OH)_2$] and MG262 [Z-LLL-B$(OH)_2$]. Boronic acid derivatives directly block the hydroxyl group, occupy the binding pocket and increase basicity of the catalytic amine in serine or threonine proteases. The stable, anionic covalent adduct formed by boronic acids closely resembles the transition-state tetrahedral complex created during peptide bond hydrolysis (Figure 3, Figure S2) (Groll et al., 2006;Transue et al., 2004). Binding of bortezomib or MG262 caused proteasomes to switch their conformations from mostly closed to mostly open in a dose-dependent manner (Table 1, experiment 10 and Figure 1B,C; Figure 2C). These results suggest that formation of a tetrahedral transition state during peptide bond cleavage, which is mimicked by the boronic acid adduct, is linked to the conformational shift from closed to open proteasomes.

In summary, these results point to a tetrahedral reaction intermediate as a key allosteric factor promoting α-ring opening. Since occupancy of the substrate-binding pocket or blocking the Thr1 hydroxyl group was insufficient for stimulating the conformational shift, we turned our attention to the N-terminal amino group.

Engagement of the catalytic Thr1 α amine is coupled to gate opening

None of the available proteasome inhibitors exclusively targets the α-amino group of any catalytic N-terminal threonine. However, we could take advantage of the previous observation that the propeptides of active β subunits are needed to protect the Thr1 catalytic dyad from N^{α}-acetylation during protein synthesis. The propeptides are cleaved off during proteasome assembly, when the exposed threonines are concealed within the newly formed catalytic chamber and thus no longer accessible to acetyltransferases (Arendt and Hochstrasser, 1999). As was established before, in yeast strains with a mutation that deleted a particular β-subunit propeptide sequence, the N^{α}-acetyltransferase Nat1-Ard1 specifically modified the α-amino group of the exposed Thr1 (Figure S2; Arendt and Hochstrasser, 1999). Acetylation of Thr1

NIH-PA Author Manuscript

NIH-PA Author Manuscript

NIH-PA Author Manuscript

abolishes catalytic activity of the affected active center. For example, deletion of the β1 propeptide in the *β1ΔLS* mutant strain MHY1377 resulted in almost complete (as proved with N-terminal peptide sequencing [Arendt and Hochstrasser, 1999] and mass spectrometry; data not shown) N^{α}-acetylation of β1-Thr1 and loss of all detectable PGPH activity (Arendt and Hochstrasser, 1999). As reported before, PGPH activity was fully restored by elimination of the Nat1 acetyltransferase subunit (*β1ΔLS nat1Δ*; MHY1373; Arendt and Hochstrasser, 1999).

Remarkably, when assayed by AFM, β1ΔLS mutant proteasomes, in which β1-Thr1 is N^{α}-acetylated, were nearly all in the open conformation (MHY1377, Figure 1B,C, Figure 2C–a). In contrast, β1ΔLS proteasomes isolated from cells lacking Nat1 (MHY1373) again showed the wild type ratio of conformers (mostly closed; Figure 2C–b). Deletion of Nat1 in cells with wild-type proteasomes did not influence the partitioning of conformers (MHY1372; Figure 2C–e). If the α-amino group, but not the hydroxyl of Thr1, was pivotal in the allosteric transition, proteasomes with a substitution of the β1ΔLS Thr1 with Ala (β1Δ*LS-T1A* MHY2267) should behave the same as β1ΔLS proteasomes because an N-terminal alanine is also a favored target for Nat1-Ard1 (Polevoda et al., 1999). Indeed, we found that these proteasomes were always open (Figure 2C–c), and the shift was again reversed by deletion of Nat1 (MHY2271; Figure 2C–d). Interestingly, the relative abundance of open conformers correlated closely with the degree of acetylation of the N-terminal residue of different catalytic β subunits (see Supplemental Data). From these results, we conclude that the irreversible acetylation of the α-amino group of an active site residue induces a permanent opening of the proteasome α ring.

In order to test whether the observed opening correlates with functional parameters of the particles, we tested the ability of wild-type (WT) and mutant 20S proteasomes (CPs) to be functionally activated, and compared the results with the partitioning between open and closed conformers. As a measure of functional activation we used the rate of degradation of SucLLVY-MCA (ChT-L activity). As an activating agent we chose the human 11S REG/PA28αβ ("PA28") activator complex. A homolog of PA28 was proved to open the gate of the yeast CP, and to increase the rate of degradation of SucLLVY-MCA (Whitby et al., 2000). Interestingly, the "open-gate" mutants ("morphologically activated") were refractory to functional activation with PA28 (Figure 2C). In contrast, SucLLVY-MCA cleavage by WT CPs or mutant CPs that had mostly closed-gate conformers was activated upon addition of PA28 (Figure 2C). This result links our structural observations with the functional properties of the CP. It is worth noting that active site-affecting treatments or mutations that shift the CP toward the open state do not generally cause significant activation of the remaining unaltered sites (Figure 2C and data not shown). As shown previously (Myung et al., 2001), peptide substrates for one catalytic site can inhibit activity at the other catalytic centers by a still unknown allosteric mechanism. Thus, a complex set of allosteric interactions occurs in the proteasome, making it difficult to predict the exact functional consequences of altering a particular active center. This does not amend the conclusion of specific allosteric coupling between active sites and the α-ring gate.

In apparent contradiction to our AFM findings, crystal structure-based models of eukaryotic 20S proteasomes with an intact α-ring gate display exclusively closed particles even when they had been treated with epoxomicin (Groll et al., 2000b), bortezomib (Groll et al., 2006) or had the Thr1 amine acetylated (Loidl et al., 1999), all treatments that led to preferred α-ring opening in the AFM analyses. This difference might reflect the influence of physical constraints on proteasome conformation imposed by crystal packing forces. In an attempt to mimic the confinement of particles in the crystal lattice, we examined the relative abundance of different proteasome conformers deposited on mica at higher densities. Whenever proteasomes were deposited at a density ensuring minimal contacts among the particles, the abundance of the

NIH-PA Author Manuscript

NIH-PA Author Manuscript

NIH-PA Author Manuscript

open conformer stayed close to the expected 25% for the control (Table 1) and was almost 100% for proteasomes with N^{α}-acetylated β1-Thr1 (MHY1377, Figure 1B,C; Figure 2C–a). Increasing the density to a tightly packed monolayer of proteasomes reduced these values to 8% ± 2.9% for the control (n=30 fields with 1084 top-view particles) and to only 16.0% ± 5.7% for MHY1377 proteasomes (n=35 fields, 1081 particles). These results strongly suggested that tight packing of proteasomes hampers the opening of the α-ring gate. This was further supported by the results of Thess et al. (2002), where AFM analysis of 20S proteasomes close-packed in a two-dimensional crystal monolayer revealed that the molecules were exclusively in the closed conformation.

Collectively, our AFM analyses suggest that the presence of an uncharged primary amino group on the N-terminal residue in the active center favors a closed conformation in the α-ring. This is the state of the N^{α}-amino group in "idle" proteasomes and in proteasomes blocked with lactacystin or a peptide vinyl sulfone (Table 1). In contrast, formation of a secondary amine, either by its acetylation or reaction with epoxyketone (but not by blocking with a propeptide; see Discussion), correlates with a shift toward the open conformation (Table 1). A similar preference is observed when the threonyl amine turns strongly basic during tetrahedral intermediate formation (Figure 1B,C, Figure 2B, Figure 3). We propose that the departure from the neutral primary amine status leads to structural rearrangement of the active center or its immediate surroundings, triggering an allosteric opening of the α-ring channel (Figure 3).

DISCUSSION

The present work has revealed a striking coupling between the proteasome β-subunit active centers and the opening and closing of the α-ring channel. Substrate engagement at any of the three different pairs of active sites results in a much higher proportion of particles with an open α-ring. Systematic studies of inhibitor-proteasome complexes and yeast active-site mutants indicate that the allosteric signal is linked to the α-amino group of the catalytic Thr1 residue. We infer that a tetrahedral transition state, which occurs during the proteasome reaction cycle, initiates local conformational changes that eventually propagate to the α-ring gate.

Conformational diversity of the proteasome core particle

The characteristic cylindrical shape of core particles facilitated their identification in AFM images, either as particles standing on their α-ring end or lying on their side. By AFM, *S. cerevisiae* proteasomes were indistinguishable from *S. pombe* or human complexes (Gaczynska et al., 2003; Osmulski and Gaczynska, 2000). The proteasomes were attached to the mica surface at a concentration sufficiently low to allow complete separation of the individual particles. This contrasts with other studies in which a dense layer of particles was created when His-epitope tagged proteasomes were arrayed on a derivatized surface (Dorn et al., 1999). Although such dense immobilization tends to enforce a favored orientation of the packed molecules, it limits the ability to analyze single molecules (Dorn et al., 1999; Furuike et al., 2003). By contrast, our approach allowed straightforward particle recognition and dimensioning without the need for modification or enforced placement on the surface. Our measurements of proteasome dimensions agree very well with those from published crystallographic data (Groll et al., 1997). Therefore, we conclude that AFM imaging of untagged proteasomes imaged at low density accurately depicts the topography of the yeast proteasome.

Latent yeast proteasomes, although attached to a mica surface, still switched continually between states in which the central pore in the α-ring was either open or closed in end-on views. The cycles of opening and closing resemble anharmonic fluctuations since they did not follow any detectable pattern when individual proteasomes were monitored for an extended period. There also was no observable tendency among the proteasomes to synchronize their gate

NIH-PA Author Manuscript

NIH-PA Author Manuscript

NIH-PA Author Manuscript

cycling. However, on average, ~75% of the wild-type complexes were in the closed conformation, similar to other eukaryotic proteasomes (Gaczynska and Osmulski, 2008). The less abundant open conformer is presumably less stable and as a result, shortlived in comparison to the more prevalent closed conformer. This hypothesis is strengthened by our recent data suggesting that the millisecond-scale lifetime of the closed form is three times longer than the lifetime of the open form (Osmulski and Gaczynska, unpublished observations).

It was initially puzzling that the open proteasome conformation clearly distinguished in AFM images had not been detected in crystal structures of wild-type proteasomes (Groll et al., 1997). One plausible explanation is that the closed state, which is already more stable in solution than the open state, is further stabilized by the crystal lattice. Indeed, our previous results suggest that the transition from the open to closed state is not restricted to a small section of the α-ring, but rather, is accompanied by a change in the overall shape of the particle (Osmulski and Gaczynska, 2002). Very recently, a pronounced widening of the α-ring in the 20S proteasome was detected by electron microscopy upon binding of the 19S RP, which opens the central gate (da Fonseca and Morris, 2008). Proteasomes immobilized in a crystal lattice may not have enough energy to achieve such a structural transition. In agreement with this idea, more densely packed proteasomes deposited on mica exhibit a greatly decreased tendency to switch out of the closed conformation. Moreover, proteasomes with an acetylated catalytic N-terminus, which were classified in AFM images as being almost entirely open when deposited at low concentration, apparently closed the gate in more than 80% of particles when analyzed as a densely packed layer. These data are also consistent with the possibility that α-ring gate opening is coupled with a global conformational change of the β rings. Interestingly, conformational fluctuations of proteins were found to be impeded by molecular crowding based on a combination of X-ray scattering and computational modeling (Makowski et al., 2008).

Conformational transitions are necessary for catalytic activity of the proteasome

The proteasome is by no means unique in its structural dynamics. Conformational diversity is likely to be a common if not universal property of proteins (Bahar et al., 2007). Such intrinsic, thermodynamically driven motions can be harnessed to achieve catalytic proficiency in enzymes (Bahar et al., 2007; Henzler-Wildman et al., 2007). Closed and open conformations are evident in many multisubunit assemblies with cylindrical or ring structures, such as chaperones, membrane channels, and receptors (Muller and Engel, 1999; Schoehn et al., 2000; Stolz et al., 2000). With up to 25% of particles showing an alternative conformer, proteasomal open and closed conformers must have a rather small free energy difference. The relatively high probability of latent proteasomes switching to a state allowing access to the catalytic chamber explains the well-documented ability of latent CP to hydrolyze substrates. A dynamic gate in the α-ring would allow an unfolded protein or protein domain to enter the CP without involvement of the 19S RP or other components of the ubiquitin system. This has in fact been documented with intrinsically unfolded proteins (Liu et al., 2003). The low, but measurable rates of degradation of model peptide substrates or denatured polypeptides commonly observed with latent eukaryotic CPs can also be explained by a stochastic opening of the α-ring gate (Bajorek et al., 2003; Rosenzweig et al., 2008). Previously, the activity of latent CP against certain hydrophobic peptides or unfolded domains was proposed to derive from their direct interaction with the α-ring, promoting gate opening “from the outside” (Kisselev et al., 2002; Liu et al., 2003). Although plausible, this model applies to only a subset of substrates and requires the existence of specific receptor sites in the α ring. The conformational diversity hypothesis explains activity toward all CP substrates without evoking additional structural features.

Proteasomes treated with substrates, both short peptides and denatured proteins, retain the ability to switch between open and closed states, and the respective conformers are

NIH-PA Author Manuscript

NIH-PA Author Manuscript

NIH-PA Author Manuscript

indistinguishable from those observed in the absence of ligands. However, exposure to a degradable polypeptide shifts the conformational equilibrium toward the open conformer (Osmulski and Gaczynska, 2000). The shift is fully reversible by washing out the substrate from the reaction mixture (Osmulski and Gaczynska, 2002). Here we confirm that the cognate active center has to be fully functional for this effect. Any mutational disruption or chemical modification with active-site inhibitors prevents the equilibrium shift. Moreover, our preliminary findings show that with substrate concentrations below the steady-state conditions, the shift was reversed with time: a strong suggestion of substrate depletion (Osmulski and Gaczynska, unpublished observations). Finally, we note that our model of active site-regulated proteasome dynamics is not in conflict with previously postulated noncatalytic allosteric sites (Myung et al., 2001; Schmidtke et al., 2000). Indeed, such interactions can be invoked to explain the strong activating effect of certain hydrophobic peptides on substrate hydrolysis without the need of gate opening “from the outside” by these peptides (Kisselev et al., 2002).

The α-amino group of the catalytic Thr residue is a central allosteric effector

Previously, we had hypothesized that the relative abundance of the two detectable proteasome conformations might be related to proteasomal catalytic activity (Osmulski and Gaczynska, 2000, 2002). Our new AFM data reveal a clear coupling between the CP active centers and α-ring conformation. Such coupling is consistent with recent observations suggesting that changes in the stability of CP-RP interactions correlate with changes in catalytic chamber engagement (Kleijnen et al., 2007). Our analysis of proteasomes exposed to reagents modifying specific elements of the active centers and examination of yeast active-site mutants point to the tetrahedral transition state as the most probable initiator of the conformational switch. Transition state-related structural changes in the active center are proposed to trigger a cascade of conformational alterations leading to the opening of the remote α-ring gate. Slow, millisecond-scale conformational transitions connected to catalytic cycles have been reported for a variety of enzymes (Hammes-Schiffer and Benkovic, 2006). In general, the observed activity-related motions on a microsecond-to-millisecond time scale fit the concept of conformational sampling performed by enzymes to optimize catalysis (Bahar et al., 2007).

A search for specific molecular elements in the active center that were potentially involved in conformational signaling fingered the Thr1 α-amino group as the strongest candidate for the allosteric trigger (Table 1, Figure 4). We observed a dramatic shift of the conformational equilibria toward the open form when the α-amine was engaged by a substrate, a transition state analog, epoxyketone inhibitors, or an acetyl group. All of these compounds react with Thr1 in a way that either creates a secondary amine or substantially increases the basicity of the primary amine (Figure 4). By analogy to serine proteases, whose catalytic mechanism is closely related to that of the proteasome, these changes should cause subtle but significant structural remodeling of the active center (Groll et al., 2006;Radisky et al., 2006). We therefore propose that alteration of the a amine of Thr1 is the proximate trigger for the conformational switch that culminates many nanometers away at the proteasome gate.

Studies on allosteric signaling have suggested that the transmission of signals over long distances is based on reorganization of hydrogen bonds or, less often, salt bridges (for example: Begg et al., 2006; Guallar et al., 2006; Yun et al., 2007). Sometimes breaking just a single hydrogen bond is sufficient to initiate a cascade of allosteric changes, as in the *E. coli* purine repressor (Lu et al., 1998). In another example, coupling between local conformational fluctuations, proton binding, and global structural motions was described for Staphylococcal nuclease (Whitten et al., 2005).

By analogy, we propose that changes to the proteasome Thr1 α-amine are translated into a set of adaptations within the active site hydrogen-bonding network, which is eventually transmitted into a structural remodeling of the proteasome gate. Thermally induced

NIH-PA Author Manuscript

NIH-PA Author Manuscript

NIH-PA Author Manuscript

rearrangements of hydrogen bonds in the active center of "idle" proteasome may mimic the transition state-like configuration and thereby support a significantly populated open gate state (25%). This model can accommodate the one known discrepancy in the correlation between Thr1 a amine modification and gate opening. Specifically, in the β1T1A proteasome, which still retains a β1 propeptide remnant in the substrate binding pocket and therefore has a modified amine at Ala1, the α-ring gate is nevertheless closed both in the crystal structure (Groll et al., 1997) and in the majority of particles analyzed by AFM (Figure 2C, Table 1). The distinct geometry of the propeptide extending beyond the active center, in combination with the unique organization of surrounding hydrogen bonds, disables the expected shift toward the predominantly open conformer (Osmulski, Hochstrasser, Gaczynska, in preparation).

Studies are underway to test the proposed role of remodeling of the hydrogen-bond network in the active site vicinity as a source of the observed gate opening. We are also exploring the allosteric pathways leading from the active centers to the α-ring gate. Ultimately, a combination of AFM, high-resolution crystallography, mutational, and biochemical studies will be needed to derive a complete picture of the dynamic processes linking the proteasome active sites and its gated entry channels.

EXPERIMENTAL PROCEDURES

Construction of yeast strains

Most of the yeast strains used were described previously (Arendt and Hochstrasser, 1997, 1999; Chen and Hochstrasser, 1996), and others are discussed in Supplemental Data.

Purification of 20S proteasomes and activity measurements

Latent 20S proteasomes were isolated from exponentially growing cultures of *Saccharomyces cerevisiae* in YPD medium (see Supplemental Data). Activity measurements were performed with one of three commonly used fluorogenic peptide substrates, as outlined in Supplemental Data.

Imaging with atomic force microscopy (AFM)

The imaging was performed in tapping mode in liquid, as described previously (Osmulski and Gaczynska, 2000) and in Supplemental Data. Standard plane fits provided by the NanoScope IIIa software (v. 5.1) were the only processing procedures applied to the images of the whole 1 μm^2 fields in the height mode.

Distinguishing and counting conformers in AFM images

In our previous studies, we found that 20S proteasomes imaged with AFM had two conformations, representing an open or closed entrance to the central channel (summarized in Gaczynska and Osmulski, 2008). They were distinguished by the qualitative shape of the median sections of particles in top-view orientation (Osmulski and Gaczynska, 2000; Supplemental Data). In short, median sections (density profiles) of the particles were analyzed with section-analysis software (Veeco). Only if all the sections were crater-shaped, with a depression in the middle of the α-ring, the particle was counted as open (Figure 1B).

Supplementary Material

Refer to Web version on PubMed Central for supplementary material.

Acknowledgements

This work was supported by NIH grants R01 GM069819 (M.G.) and R01 GM083050 (M.H.).

NIH-PA Author Manuscript

NIH-PA Author Manuscript

NIH-PA Author Manuscript

References

Arendt CS, Hochstrasser M. Identification of the yeast 20S proteasome catalytic centers and subunit interactions required for active-site formation. Proc. Natl Acad. Sci. USA 1997;94:7156–7161. [PubMed: 9207060]

Arendt CS, Hochstrasser M. Eukaryotic 20S proteasome catalytic subunit propeptides prevent active site inactivation by N-terminal acetylation and promote particle assembly. EMBO J 1999;18:3575–3585. [PubMed: 10393174]

Bahar I, Chennubhotla C, Tobi D. Intrinsic dynamics of enzymes in the unbound state and relation to allosteric regulation. Curr. Opinion Struct. Biol 2007;17:633–640.

Bajorek M, Finley D, Glickman MH. Proteasome disassembly and downregulation is correlated with viability during stationary phase. Curr. Biol 2003;13:1140–1144. [PubMed: 12842014]

Begg GE, Carrington L, Stokes PH, Matthews JM, Wouters MA, Husain A, Lorand L, Iismaa SE, Graham RM. Mechanism of allosteric regulation of transglutaminase 2 by GTP. Proc. Natl Acad. Sci. USA 2006;103:19683–19688. [PubMed: 17179049]

Bogyo M, McMaster JS, Gaczynska M, Tortorella D, Goldberg AL, Ploegh H. Covalent modification of the active site threonine of proteasomal beta subunits and the Escherichia coli homolog HslV by a new class of inhibitors. Proc. Natl Acad. Sci. USA 1997;94:6629–6634. [PubMed: 9192616]

Chen P, Hochstrasser M. Autocatalytic subunit processing couples active site formation in the 20S proteasome to completion of assembly. Cell 1996;86:961–972. [PubMed: 8808631]

Corey EJ, Li WDZ, Nagamitsu T, Fenteany G. The structural requirements for inhibition of proteasome function by the lactacystin-derived beta-lactone and synthetic analogs. Tetrahedron 1999;55:3305–3316.

da Fonseca PCA, Morris EP. Structure of the human 26S proteasome: subunit radial displacements open the gate into the proteolytic core. J. Biol. Chem 2008;283:23305–23314. [PubMed: 18534977]

Dodson GG, Lane DP, Verma CS. Molecular simulations of protein dynamics: New windows on mechanisms in biology. EMBO Reports 2008;9:144–150. [PubMed: 18246106]

Dorn IT, Eschrich R, Seemuller E, Guckenberger R, Tampe R. High-resolution AFM-imaging and mechanistic analysis of the 20 S proteasome. J. Mol. Biol 1999;288:1027–1036. [PubMed: 10329196]

Elofsson M, Splittgerber U, Myung J, Mohan R, Crews CM. Towards subunit-specific proteasome inhibitors: synthesis and evaluation of peptide alpha ',beta '-epoxyketones. Chemistry & Biology 1999;6:811–822. [PubMed: 10574782]

Forster A, Whitby FG, Hill CP. The pore of activated 20S proteasomes has an ordered 7-fold symmetric conformation. EMBO J 2003;22:4356–4364. [PubMed: 12941688]

Furuike S, Hirokawa J, Yamada S, Yamazaki M. Atomic force microscopy studies of interaction of the 20S proteasome with supported lipid bilayers. Biochim. Biophys. Acta (BBA) - Biomembranes 2003;1615:1–6.

Gaczynska M, Osmulski PA. AFM of biological complexes: what can we learn? Curr Opinion Colloid Interface Sci 2008;13:351–367.

Gaczynska M, Osmulski PA, Gao Y, Post MJ, Simons M. Proline- and arginine-rich peptides constitute a novel class of allosteric inhibitors of proteasome activity. Biochemistry 2003;42:8663–8670. [PubMed: 12873125]

Glickman MH, Ciechanover A. The ubiquitin-proteasome proteolytic pathway: destruction for the sake of construction. Physiol. Rev 2002;82:373–428. [PubMed: 11917093]

Groll M, Bajorek M, Kohler A, Moroder L, Rubin DM, Huber R, Glickman MH, Finley D. A gated channel into the proteasome core particle. Nature Struct. Biol 2000a;7:1062–1067. [PubMed: 11062564]

Groll M, Berkers CR, Ploegh HL, Ovaa H. Crystal structure of the boronic acid-based proteasome inhibitor bortezomib in complex with the yeast 20S proteasome. Structure 2006;14:451–456. [PubMed: 16531229]

Groll M, Ditzel L, Lowe J, Stock D, Bochtler M, Bartunik HD, Huber R. Structure of 20S proteasome from yeast at 2.4 A resolution. Nature 1997;386:463–471. [PubMed: 9087403]

NIH-PA Author Manuscript NIH-PA Author Manuscript NIH-PA Author Manuscript

Groll M, Kim KB, Kairies N, Huber R, Crews CM. Crystal structure of epoxomicin : 20S proteasome reveals a molecular basis for selectivity of alpha ',beta '-epoxyketone proteasome inhibitors. J. Am. Chem. Soc 2000b;122:1237–1238.

Guallar V, Jarzecki AA, Friesner RA, Spiro TG. Modeling of ligation-induced helix/loop displacements in myoglobin: Toward an understanding of hemoglobin allostery. J. Am. Chem. Soc 2006;128:5427–5435. [PubMed: 16620114]

Gunasekaran K, Ma B, Nussinov R. Is allostery an intrinsic property of all dynamic proteins? Proteins 2004;57:433–443. [PubMed: 15382234]

Hammes-Schiffer S, Benkovic SJ. Relating protein motion to catalysis. Annu Rev. Biochem 2006:519–541. [PubMed: 16756501]

Heinemeyer W, Fischer M, Krimmer T, Stachon U, Wolf DH. The active sites of the eukaryotic 20 S proteasome and their involvement in subunit precursor processing. J. Biol. Chem 1997;272:25200–25209. [PubMed: 9312134]

Henzler-Wildman KA, Thai V, Lei M, Ott M, Wolf-Watz M, Fenn T, Pozharski E, Wilson MA, Petsko GA, Karplus M, et al. Intrinsic motions along an enzymatic reaction trajectory. Nature 2007;450:838–844. [PubMed: 18026086]

Kisselev AF, Kaganovich D, Goldberg AL. Binding of hydrophobic peptides to several non-catalytic sites promotes peptide hydrolysis by all active sites of 20 S proteasomes - Evidence for peptide-induced channel opening in the alpha-rings. J. Biol. Chem 2002;277:22260–22270. [PubMed: 11927581]

Kleijnen MF, Roelofs J, Park S, Hathaway NA, Glickman M, King RW, Finley D. Stability of the proteasome can be regulated allosterically through engagement of its proteolytic active sites. Nature Struct. Mol. Biol 2007;14:1180–1188. [PubMed: 18026118]

Liu CW, Corboy MJ, DeMartino GN, Thomas PJ. Endoproteolytic activity of the proteasome. Science 2003;299:408–411. [PubMed: 12481023]

Liu YH, Konermann L. Conformational dynamics of free and catalytically active thermolysin are indistinguishable by hydrogen/deuterium exchange mass spectrometry. Biochemistry 2008;47:6342–6351. [PubMed: 18494500]

Loidl G, Groll M, Musiol HJ, Ditzel L, Huber R, Moroder L. Bifunctional inhibitors of the trypsin-like activity of eukaryotic proteasomes. Chemistry & Biology 1999;6:197–204. [PubMed: 10099130]

Lu F, Brennan RG, Zalkin H. Escherichia coli purine repressor: Key residues for the allosteric transition between active and inactive conformations and for interdomain signaling. Biochemistry 1998;37:15680–15690. [PubMed: 9843372]

Makowski L, Rodi DJ, Mandava S, Minh DDL, Gore DB, Fischetti RF. Molecular Crowding Inhibits Intramolecular Breathing Motions in Proteins. J. Mol. Biol 2008;375:529–546. [PubMed: 18031757]

Muller DJ, Engel A. Voltage and pH-induced channel closure of porin OmpF visualized by atomic force microscopy. J. Mol. Biol 1999;285:1347–1351. [PubMed: 9917378]

Myung J, Kim KB, Lindsten K, Dantuma NP, Crews CM. Lack of proteasome active site allostery as revealed by subunit-specific inhibitors. Mol. Cell 2001;7:411–420. [PubMed: 11239469]

Nevo R, Brumfeld V, Elbaum M, Hinterdorfer P, Reich Z. Direct Discrimination between Models of Protein Activation by Single-Molecule Force Measurements. Biophys. J 2004;87:2630–2634. [PubMed: 15454457]

Osmulski PA, Gaczynska M. Atomic force microscopy reveals two conformations of the 20 S proteasome from fission yeast. J. Biol. Chem 2000;275:13171–13174. [PubMed: 10747864]

Osmulski PA, Gaczynska M. Nanoenzymology of the 20S proteasome: proteasomal actions are controlled by the allosteric transition. Biochemistry 2002;41:7047–7053. [PubMed: 12033938]

Osmulski, PA.; Tokmina-Lukaszewska, M.; Endel, L.; Sosnowska, R.; Gaczynska, M. Wiley Encyclopedia of Chemical Biology. John Wiley and Sons, Inc.; 2008. Chemistry of proteasome.

Polevoda B, Norbeck J, Takakura H, Blomberg A, Sherman F. Identification and specificities of N-terminal acetyltransferases from Saccharomyces cerevisiae. EMBO J 1999;18:6155–6168. [PubMed: 10545125]

Radisky ES, Lee JM, Lu CJK, Koshland DE Jr. Insights into the serine protease mechanism from atomic resolution structures of trypsin reaction intermediates. Proc. Natl Acad. Sci. USA 2006;103:6835–6840. [PubMed: 16636277]

NIH-PA Author Manuscript

NIH-PA Author Manuscript

NIH-PA Author Manuscript

Rechsteiner M, Hill CP. Mobilizing the proteolytic machine: Cell biological roles of proteasome activators and inhibitors. Trends Cell Biol 2005;15:27–33. [PubMed: 15653075]

Rosenzweig R, Osmulski PA, Gaczynska M, Glickman M. The central unit within the 19S regulatory particle of the proteasome. Nature Struct. Mol. Biol 2008;15:573–580. [PubMed: 18511945]

Schmidtke G, Emch S, Groettrup M, Holzhutter HG. Evidence for the existence of a non-catalytic modifier site of peptide hydrolysis by the 20 S proteasome. J. Biol. Chem 2000;275:22056–22063. [PubMed: 10806206]

Schmidtke G, Kraft R, Kostka S, Henklein P, Frommel C, Lowe J, Huber R, Kloetzel PM, Schmidt M. Analysis of mammalian 20S proteasome biogenesis: the maturation of beta-subunits is an ordered two-step mechanism involving autocatalysis. EMBO J 1996;15:6887–6898. [PubMed: 9003765]

Schoehn G, Hayes M, Cliff M, Clarke AR, Saibil HR. Domain rotations between open, closed and bullet-shaped forms of the thermosome, an archaeal chaperonin. J. Mol. Biol 2000;301:323–332. [PubMed: 10926512]

Seemuller E, Lupas A, Baumeister W. Autocatalytic processing of the 20S proteasome. Nature 1996;382:468–471. [PubMed: 8684489]

Smith DM, Chang SC, Park S, Finley D, Cheng Y, Goldberg AL. Docking of the Proteasomal ATPases' Carboxyl Termini in the 20S Proteasome's a Ring Opens the Gate for Substrate Entry. Mol. Cell 2007;27:731–744. [PubMed: 17803938]

Sprangers R, Kay LE. Quantitative dynamics and binding studies of the 20S proteasome by NMR. Nature 2007;445:618. [PubMed: 17237764]

Stolz M, Stoffler D, Aebi U, Goldsbury C. Monitoring biomolecular interactions by time-lapse atomic force microscopy. J. Struct. Biol 2000;131:171–180. [PubMed: 11052889]

Tang M, Cecconi C, Bustamante C, Rio DC. Analysis of P element transposase protein-DNA interactions during the early stages of transposition. J. Biol. Chem 2007;282:29002–29012. [PubMed: 17644523]

Thess A, Hutschenreiter S, Hofmann M, Tampe R, Baumeister W, Guckenberger R. Specific orientation and two-dimensional crystallization of the proteasome at metal-chelating lipid interfaces. J. Biol. Chem 2002;277:36321–36328. [PubMed: 12114506]

Transue TR, Krahn JM, Gabel SA, DeRose EF, London RE. X-ray and NMR Characterization of Covalent Complexes of Trypsin, Borate, and Alcohols. Biochemistry 2004;43:2829–2839. [PubMed: 15005618]

Whitby FG, Masters EI, Kramer L, Knowlton JR, Yao Y, Wang CC, Hill CP. Structural basis for the activation of 20S proteasomes by 11S regulators. Nature 2000;408:115–120. [PubMed: 11081519]

Whitten ST, Garcia-Moreno EB, Hilser VJ. Local conformational fluctuations can modulate the coupling between proton binding and global structural transitions in proteins. Proc. Natl Acad. Sci. USA 2005;102:4282–4287. [PubMed: 15767576]

Yun MK, Nourse A, White SW, Rock CO, Heath RJ. Crystal Structure and Allosteric Regulation of the Cytoplasmic Escherichia coli l-Asparaginase I. J. Mol. Biol 2007;369:794–811. [PubMed: 17451745]

NIH-PA Author Manuscript

NIH-PA Author Manuscript

NIH-PA Author Manuscript

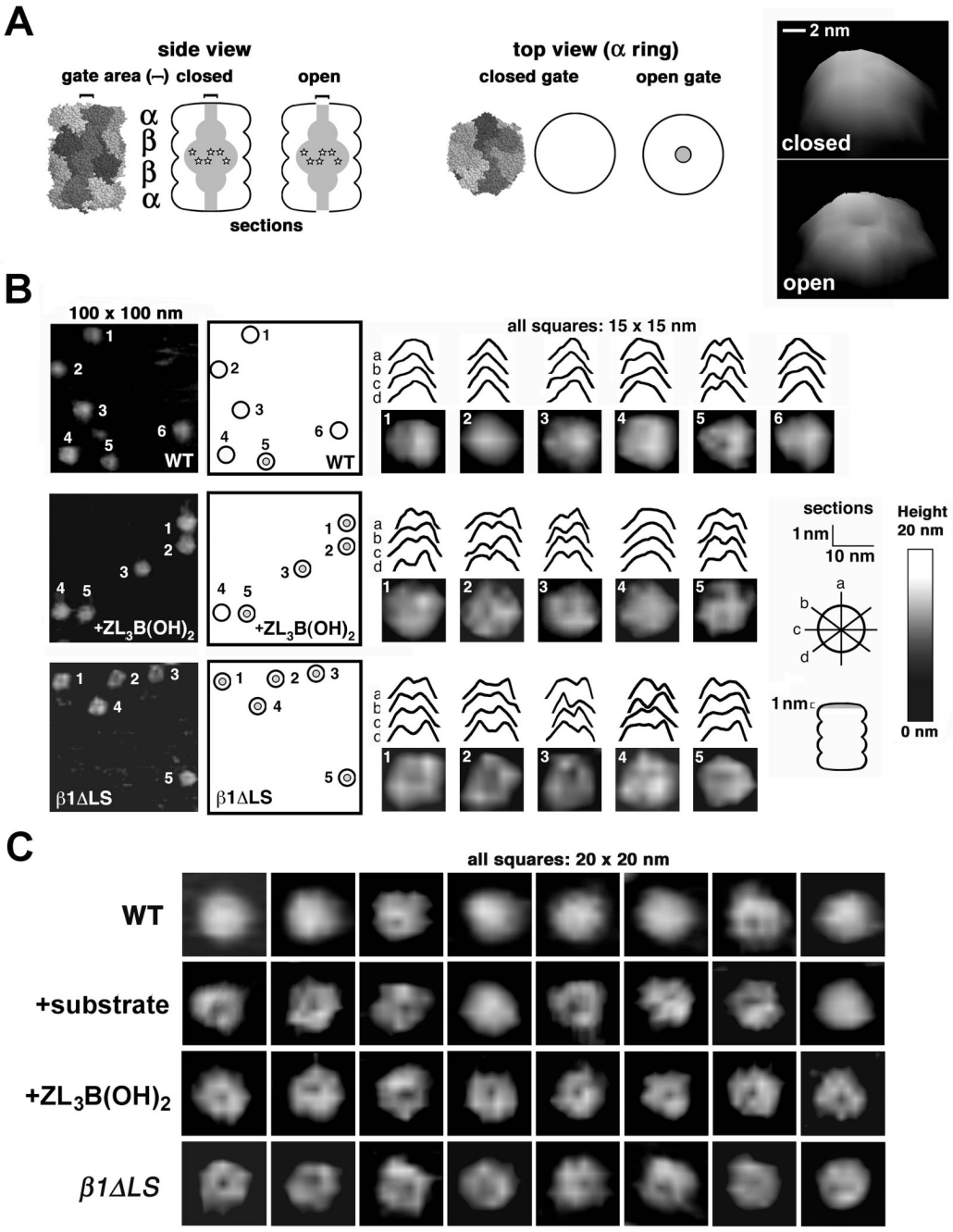

Figure 1.

The top view 20S proteasomes were detected with AFM either in open or closed conformation. (A) Left and center, the shape of 20S proteasome based on the yeast crystal structure (1ryp). From the left: side view with subunits marked with shades of grey and rings labeled, contour of the side view particle, contour of the side view section with the central channel, antechambers and catalytic chamber colored in grey, with active sites marked with stars. The gate area is marked. Center: top view of the α-ring (1ryp), contour of the α-ring with closed gate, contour of the α-ring with the gate open (marked as grey circle). Right: tilted view images of particles classified as closed (top) and open (bottom). (B) Classification of top view wild type (top), inhibitor treated (middle), and mutated (bottom) particles into closed and open conformers.

NIH-PA Author Manuscript

NIH-PA Author Manuscript

NIH-PA Author Manuscript

From the left: selections of proteasome fields with 5 or 6 top view particles; diagrams presenting the classification of individual proteasomes; zoomed-in images of the particles with corresponding sections through the topmost part of their a rings; diagrams demonstrating how central sections in four directions were run through the zoomed-in images of particles and (below) which part of the a ring (shaded) is sectioned. A particle is classified as open when all four sections of its a ring are showing a dip. The gray-scale bar represents the height of the particles from the baseline (black) to the top (white). The same height scale applies to images in A and C. (C) Close-ups of individual top-view WT, ligand-treated, or mutated particles. Note the presence or absence of a hole or dip (a dark central circle) in the a rings. The WT proteasomes had either an open (with a hole) or closed (rounded apical part of the α-ring) entrance to the central channel. The treatment with a ligand shifted the conformational equilibrium toward more open (substrate) or nearly all open (0.5 μM $ZL_3B(OH)_2$) particles. The mutated proteasomes shown (β*1*Δ*LS*; MHY1377; Arendt and Hochstrasser, 1999) were always in the open-channel state.

NIH-PA Author Manuscript

NIH-PA Author Manuscript

NIH-PA Author Manuscript

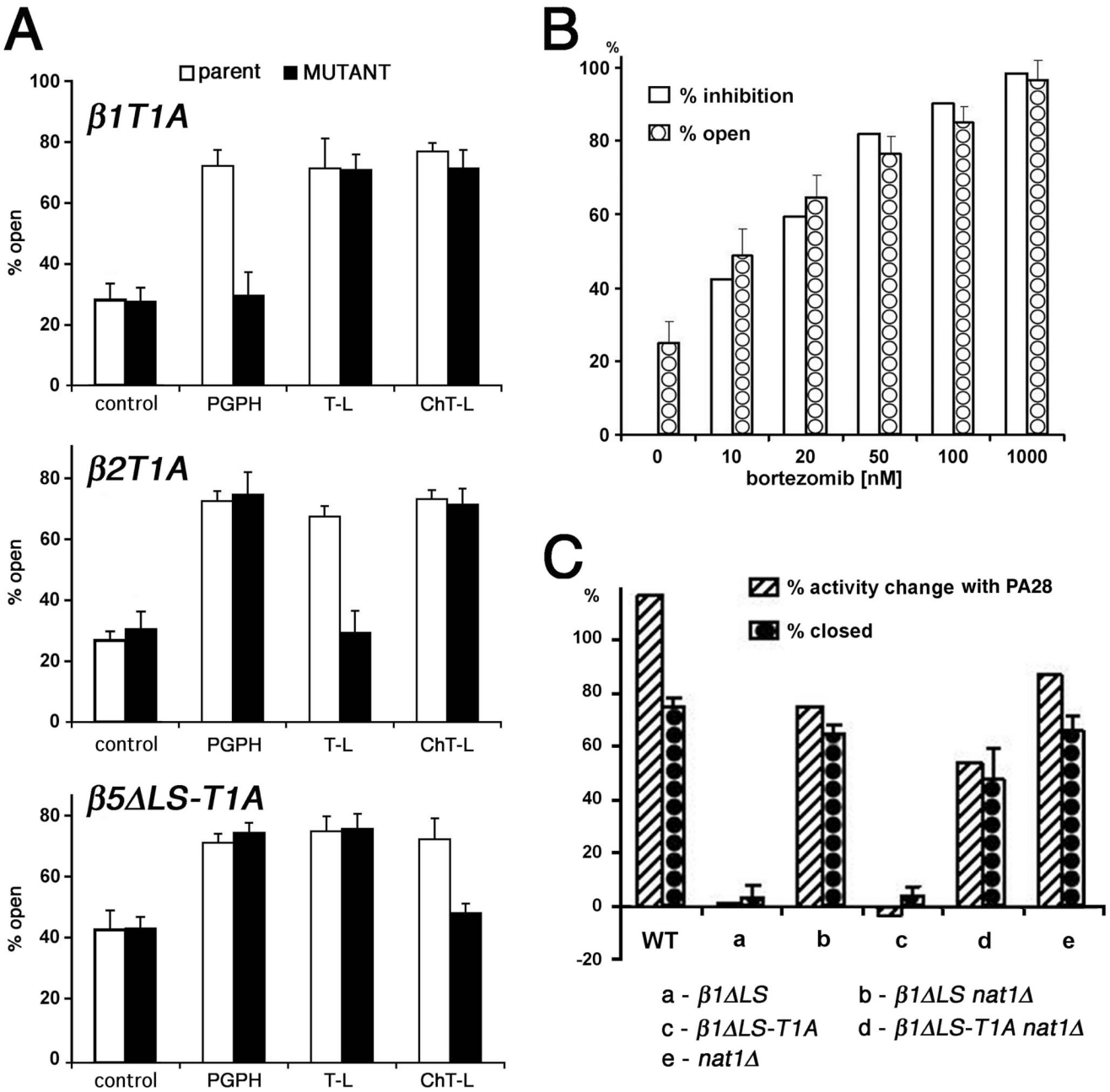

Figure 2.

The chemical state of the active center determines the conformation of the gate.

(A) A functional active site is essential to trigger the substrate-induced shift in the conformational equilibrium of 20S proteasomes. Proteasomes were isolated from yeast strains in which the indicated catalytic threonine (Thr1) was substituted with alanine. The mutants were specifically devoid of one of the following activities: PGPH (post-acidic) (β*1T1A*, MHY1157), T-L (trypsin like, β*2T1A*, MHY1073) or the ChT-L activity (chymotrypsin-like, β*5*Δ*LS-T1A*, MHY973) (Arendt and Hochstrasser, 1997). The proteasomes from the mutant and corresponding parent strains (MHY1156, MHY1066, MHY952) were imaged after addition of a buffer with solvent (DMSO; control) or after a separate addition of the substrate specific for each of the three active centers. Bars represent means ± SD calculated for n = 8 to

NIH-PA Author Manuscript

NIH-PA Author Manuscript

NIH-PA Author Manuscript

20 fields with 200 to 500 top-view particles. The differences in abundance of the conformers were statistically significant at $p<0.001$ between the control and working proteasomes, with an exception of the respective T1A proteasomes in the presence of a substrate specific for the affected site; in these cases the ratios in working and control particles were identical.

(B) Exposing proteasomes to bortezomib, an inhibitor that forms a tetrahedral transition state analogue with the ChT-L active center, induced the opening of the proteasome gate. Wild-type 20S proteasomes were imaged before and after treatment with the specified concentrations of the inhibitor. The percentage of open particles (bars with white circles) increased with the increasing concentration of the inhibitor, while the ChT-L activity (white bars) decreased. The degradation of the SucLLVY-MCA substrate (releaser of free aminomethylcoumarin; AMC) was determined spectrofluorometrically with the same sample of proteasomes, which were used for AFM imaging. Black bars represent means ± SD (n = 9 to 17 fields with 300 to 600 top-view particles).

(C) N^{α}-acetylation of catalytic subunits was accompanied by gate opening. The particles with an open gate were refractory to enhancement of their ChT-L activity by addition of 5-fold molar excess of human PA28 activator. The following 20S proteasomes were analyzed: a – β*1*Δ*LS* (MHY1377); b - β*1*Δ*LSnat1*Δ (MHY1373); c - β*1*Δ*LS-T1A* (MHY2267); d - β*1*Δ*LS-T1A nat1*Δ (MHY2271); e - *nat1*Δ (MHY1372). Bars patterned with black circles represent the percentage of closed particles without ligand addition, with means ± SD (n = 10 to 20 fields with 150 to 350 top-view proteasomes). Bars with a diagonal pattern represent the percent of ChT-L activity change upon addition of PA28 (0% change for unliganded CP). The activities of unliganded samples expressed in nanomoles of released AMC product per mg of protein per second were: WT – 0.37, a – 0.45, b – 0.33, c – 0.41, d – 0.35, e – 0.43.

NIH-PA Author Manuscript

NIH-PA Author Manuscript

NIH-PA Author Manuscript

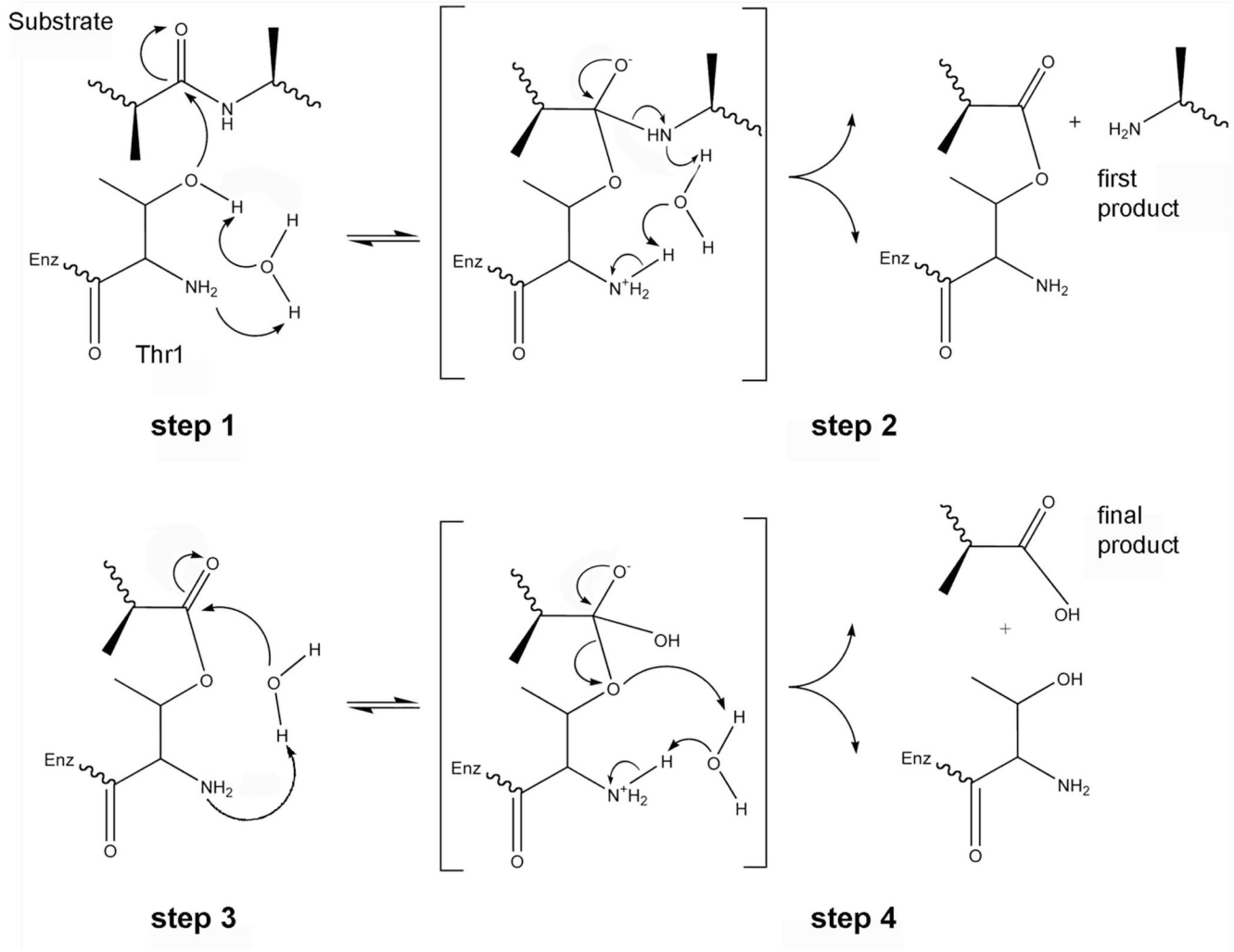

Figure 3.

Catalytic mechanism of the proteasome.

The four major steps of catalytic cycle are shown: (1) the nucleophilic attack by the Thr1 hydroxyl on the carbonyl of the peptide bond, (2) a rearrangement of a tetrahedral intermediate and release of the first product, (3) the second nucleophilic attack by a water molecule leading to a formation of a second tetrahedral complex, (4) a rearrangement of the complex and release of the final product (Groll et al., 2006; Groll et al., 1997; Osmulski et al., 2008).

NIH-PA Author Manuscript

NIH-PA Author Manuscript

NIH-PA Author Manuscript

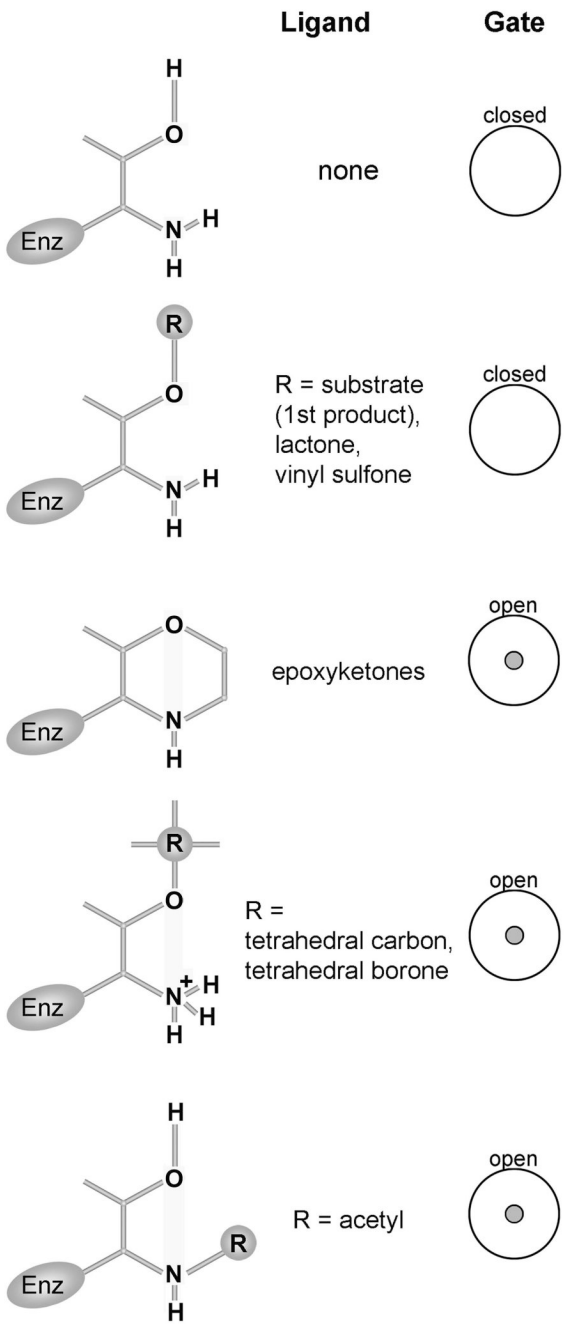

Figure 4.

Engagement of the catalytic Thr1 α amine and the open conformation of the gate are correlated. The shift toward open gate is noted when the a amine is blocked (secondary) or ionized.

Left column: schematic representation of catalytic Thr1 under distinct liganding conditions.

Middle column: the ligand used.

Right column: the prevailing conformation of the gate computed from AFM images.

NIH-PA Author Manuscript NIH-PA Author Manuscript NIH-PA Author Manuscript

Table 1

Selected competitive inhibitors dramatically shifted the conformational equilibrium toward an excess of open particles. A subunit with the active center targeted by a mutation or modified by an inhibitor was designated as "subunit affected". For the peptidase activity measurements and AFM imaging, proteasomes were exposed to the identical concentration of the inhibitors. Many of the inhibitors modify more than a single type of the active center, however with substantially different affinities. To achieve a predominant modification of only one selected active center, substantially lower concentrations of the particular inhibitor were used leading to the inhibition significantly lower than the maximum possible effect. The ChT-L (experiments 1–3 and 7–11) or post-acidic activities (experiments 4 – 6) of the proteasomes were determined in the presence and absence of the inhibitors and are expressed as % inhibition. LC - *clasto*-lactacystin β-lactone; NA - not applicable: the β1 active site was dysfunctional and the post-acidic activity not measurable in the β1T1A mutant.

	Strain MHY	Subunit affected	Mutation	Inhibitor Final concentration	% Inhibition	% of open particles (mean ± SD)	No. of fields	No. of particles
1	501	none	WT	none	0	25.4 ± 3.6	84	1877
2	501	β5	WT	Epoxomicin 1μM	94	95.6 ± 1.7	10	420
3	501	β5	WT	YU101 50 nM	74	73.4 ± 3.3	18	392
4	501	β1	WT	YU102 20 μM	77	74.5 ± 5.6	10	205
5	1157	β1	β1T1A	none	0	24.8 ± 3.7	10	150
6	1157	β1	β1T1A	YU102 20 μM	NA	27.4 ± 5.0	12	176
7	1157	β1, β5	β1T1A	YU101 50 nM	59	65.7 ± 7.0	13	294
8	501	β5	WT	ZL_3VS 50 μM	96	25.7± 3.5	12	110
9	501	β5	WT	LC 50 μM	93	25.7± 2.2	10	100
10	501	β5	WT	bortezomib. 100 nM	90	85.1± 4.2	10	86
11	501	β5	WT	MG262 0.5 μM	91	87.1± 4.7	10	157